

MulVul: Retrieval-augmented Multi-Agent Code Vulnerability Detection via Cross-Model Prompt Evolution

Anonymous ACL submission

Abstract

Large Language Models (LLMs) struggle to automate real-world vulnerability detection due to two key limitations: the heterogeneity of vulnerability patterns undermines the effectiveness of a single unified model, and manual prompt engineering for massive weakness categories is unscalable. To address these challenges, we propose **MulVul**, a retrieval-augmented multi-agent framework designed for precise and broad-coverage vulnerability detection. MulVul adopts a coarse-to-fine strategy: a *Router* agent first predicts the top- k coarse categories and then forwards the input to specialized *Detector* agents, which identify the exact vulnerability types. Both agents are equipped with retrieval tools to actively source evidence from vulnerability knowledge bases to mitigate hallucinations. Crucially, to automate the generation of specialized prompts, we design *Cross-Model Prompt Evolution*, a prompt optimization mechanism where a generator LLM iteratively refines candidate prompts while a distinct executor LLM validates their effectiveness. This decoupling mitigates the self-correction bias inherent in single-model optimization. Evaluated on 130 CWE types, MulVul achieves 34.79% Macro-F1, outperforming the best baseline by 41.5%. Ablation studies validate cross-model prompt evolution, which boosts performance by 51.6% over manual prompts by effectively handling diverse vulnerability patterns.

1 Introduction

Code vulnerabilities pose a fundamental threat to software reliability and security, leading to software crashes and service interruptions (Peng et al., 2024). As modern software systems grow in complexity, manual code auditing has become increasingly expensive, time-consuming, and error-prone, motivating the need for automated vulnerability detection (Ghaffarian and Shahriari, 2017).

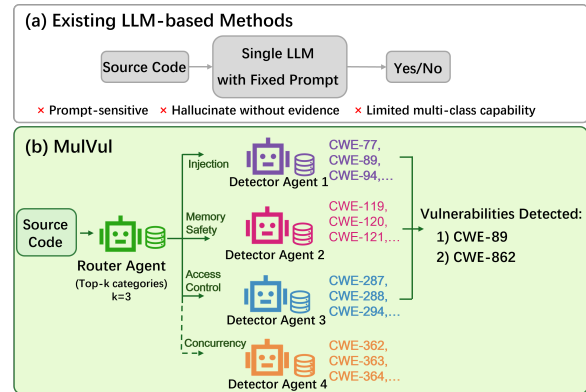


Figure 1: Comparison between MulVul and existing LLM-based vulnerability detection methods. (a) Existing methods rely on fixed prompts and lack external grounding. (b) MulVul adopts a coarse-to-fine, retrieval-augmented multi-agent framework for multi-type vulnerability detection.

Recent advances in large language models (LLMs) have sparked interest in their application to vulnerability detection (Peng et al., 2025; Zhou et al., 2025). Previous efforts primarily focused on single-model approaches, where a unified model is fine-tuned or prompted to identify all vulnerability types simultaneously (Gao et al., 2025; Lin and Mohaisen, 2025). However, vulnerability patterns are highly heterogeneous (Chakraborty et al., 2021). For example, buffer overflows require reasoning about pointer arithmetic and memory bounds, while injection attacks require tracking how untrusted inputs flow into sensitive operations. As a result, a single unified detector struggles to capture these diverse, type-specific patterns within a shared latent space, leading to missed vulnerabilities or high false alarm rates.

Inspired by the success of multi-agent systems that decompose complex tasks into specialized components (Wu et al., 2024), a question arises: *Can a multi-agent architecture enhance multi-class vulnerability detection by routing inputs to special-*

065 *ized experts?*

066 It is challenging to apply a multi-agent archi- 117
067 tecture for broad-coverage vulnerability detection. 118
068 First, it is computationally prohibitive to invoke a 119
069 specialized agent for every vulnerability type. Real- 120
070 world systems involve hundreds of Common Weak- 121
071 ness Enumeration (CWE) entries (MITRE, 2024). 122
072 To ensure comprehensive coverage, querying every 123
073 corresponding agent for each input creates an im- 124
074 practical inference burden. Second, manual prompt 125
075 engineering becomes unscalable in multi-agent archi- 126
076 tectures. Unlike unified models, each special- 127
077 ized agent requires a unique instruction to capture 128
078 distinct, fine-grained patterns of vulnerability. Man- 129
079 ually optimizing prompts for such a vast number 130
080 of agents is not feasible. Third, multi-agent LLM 131
081 systems can amplify hallucinations. Evidence of 132
082 vulnerabilities is often dispersed across complex 133
083 control flows, causing agents to reason under un- 134
084 certainty. If an individual agent hallucinates a flaw, 135
085 this error can cascade through inter-agent commu- 136
086 nication, distorting the final consensus (Hong et al., 137
087 2023).

088 To address these challenges, we propose **Mul-** 138
089 **Vul**, a retrieval-augmented multi-agent framework 139
090 equipped with cross-model prompt evolution for 140
091 vulnerability detection. Figure 1 contrasts prior 141
092 methods with MulVul. MulVul adopts a coarse- 142
093 to-fine Router-Detector architecture aligned with 143
094 the hierarchical structure of CWE (MITRE, 2024). 144
095 A *Router agent* first predicts the Top-*k* coarse 145
096 categories, and only the corresponding category- 146
097 specific *Detector agents* are invoked to identify 147
098 fine-grained vulnerability types in that category. 148
099 This selective activation drastically reduces infer- 149
100 ence costs while maintaining high recall. Crucially, 150
101 to solve the scalability bottleneck of prompt engi- 151
102 neering, MulVul employs a Cross-Model Prompt 152
103 Evolution mechanism for prompt optimization. A 153
104 generator LLM (e.g., Claude) iteratively proposes 154
105 prompt candidates, while an executor LLM (e.g., 155
106 GPT-4o) evaluates their fitness. By decoupling 156
107 prompt generation from evaluation across differ- 157
108 ent LLMs, MulVul mitigates the self-correction 158
109 bias inherent in single-model optimization, yield- 159
110 ing robust and highly specialized prompts. To fur- 160
111 ther mitigate hallucinations, agents actively query 161
112 evidence from a SCALE-structured vulnerability 162
113 knowledge base (Wen et al., 2024) to ground their 163
114 reasoning. Detectors operate in isolation to prevent 164
115 error amplification across agents. 165

116 Experiments on the PrimeVul benchmark estab-

lish MulVul as the new state-of-the-art. Evaluated across 130 CWE types, MulVul achieves a Macro-F1 of 34.79%, surpassing the best baseline by 41.5%. With cross-model prompt evolution, MulVul significantly reduces false positives, ensuring detection accuracy.

The contributions are summarized as follows:

- We propose MulVul, a novel retrieval-augmented multi-agent framework for multi-class vulnerability detection. By enabling specialized agents with tool-augmented reasoning, MulVul effectively handles vulnerability heterogeneity while balancing computational efficiency with detection coverage. 124-130
- We design a Cross-Model Prompt Evolution mechanism that automatically optimizes the prompts of specialized agents. By separating generation from execution, this approach mitigates self-correction bias and solves the scalability challenge of manual prompt engineering. 131-137
- Comprehensive experiments show that MulVul significantly outperforms baselines with a 34.79% Macro-F1. Ablation studies confirm that our evolutionary mechanism boosts performance by 51.6% over manual prompts, demonstrating its critical role in handling diverse vulnerability patterns. 138-144

2 Related Work 145

Learning-based vulnerability detection. 146
Learning-based vulnerability detection has 147
progressed from early deep learning frameworks 148
(e.g., VulDeePecker (Li et al., 2018)) to neural 149
network models that learn code representations 150
with sequence and graph encoders (Zhou et al., 151
2019; Li et al., 2021; Chakraborty et al., 2021), 152
and more recently to pre-trained code models 153
such as GraphCodeBERT (Guo et al., 2021) and 154
UniXcoder (Guo et al., 2022). Recently, LLMs 155
have dominated the field due to their strong code 156
understanding capabilities (Zhou et al., 2025). 157
However, existing single-model approaches face 158
a critical challenge: a unified detector often 159
struggles to simultaneously capture the diverse 160
and fine-grained patterns of varying vulnerability 161
types (Lin and Mohaisen, 2025; Sheng et al., 162
2025). While general-purpose multi-agent 163
frameworks (e.g., AutoGen (Wu et al., 2024), 164
MetaGPT (Hong et al., 2023)) show promise in 165

task decomposition, they have not been tailored to multi-class vulnerability detection under tight cost and reliability constraints. MulVul addresses this challenge by proposing a coarse-to-fine strategy that first performs coarse-grained routing and then type-specialized identification.

Prompt engineering and optimization for LLMs. To reduce the reliance on manual prompt engineering (Wei et al., 2022), automatic optimization strategies have emerged, treating prompt generation as a search or optimization problem, such as APE (Zhou et al., 2022), EvoPrompt (Guo et al., 2024), and OPRO (Yang et al., 2023). A major limitation of these methods is their reliance on a single backbone for both generation and evaluation, which risks overfitting to model-specific biases and limits transferability across LLMs. We address this by proposing Cross-Model Prompt Evolution, which decouples the generator and executor. This separation provides unbiased feedback, facilitating the discovery of robust instructions that generalize more effectively across vulnerability types.

Retrieval-augmented generation and hallucination mitigation. Retrieval-augmented generation (RAG) effectively grounds LLMs to mitigate hallucinations (Lewis et al., 2020), with applications extending to code completion and repair (Lu et al., 2022). However, standard code retrieval often focuses on syntactic similarity, which is insufficient for distinguishing subtle security flaws. MulVul advances this by leveraging SCALE-based structured semantic representations (Wen et al., 2024) and implementing a contrastive retrieval strategy. The Router utilizes broad evidence to identify categories, while Detectors utilize contrastive example retrieval to distinguish vulnerabilities.

3 Preliminaries and Problem Definition

3.1 Common Weakness Enumeration (CWE)

The CWE taxonomy (MITRE, 2024) organizes software vulnerabilities hierarchically. We focus on a two-level structure comprising M coarse-grained categories $\mathcal{C} = \{c_1, \dots, c_M\}$ (e.g., Memory Buffer Errors, Injection). Each category c_m contains a set of fine-grained vulnerability types \mathcal{Y}_m (e.g., CWE-119 Buffer Overflow, CWE-125 Out-of-bounds Read under Memory Buffer Errors).

We define the complete label space as $\mathcal{Y} = \{y_0, y_1, \dots, y_K\}$, where y_0 denotes non-vulnerable code and $\{y_1, \dots, y_K\} = \bigcup_{m=1}^M \mathcal{Y}_m$, where $\mathcal{Y}_1, \dots, \mathcal{Y}_M$ are pairwise disjoint.

3.2 LLM-based Code Vulnerability Detection

Given an LLM \mathcal{M} with frozen parameters, we formulate vulnerability detection as a retrieval-augmented generation task. The input consists of a code snippet $x \in \mathcal{X}$ and a textual prompt p . Since real-world code may contain multiple vulnerabilities, we adopt a multi-class formulation where the system outputs a prediction set $\hat{\mathcal{Y}} \subseteq \mathcal{Y}$. In practice, the LLM generates structured outputs (e.g., a list of predicted CWE types), which are parsed to obtain $\hat{\mathcal{Y}}$. As \mathcal{M} remains frozen, detection performance relies heavily on the prompt p , which serves as the optimizable variable.

3.3 SCALE: Structured Code Representation

To capture code semantics and execution flow, SCALE (Wen et al., 2024) constructs a Structured Comment Tree for vulnerability detection. Given source code x , SCALE uses LLMs to generate natural-language comments attached to AST nodes, then applies structured rules to encode control-flow sequences, yielding $T(x) = \text{SCALE}(x)$.

3.4 Problem Formulation

Given a code snippet $x \in \mathcal{X}$, our goal is to design a multi-agent system \mathcal{A} that outputs $\hat{\mathcal{Y}} = \mathcal{A}(x) \subseteq \mathcal{Y}$. The system should achieve: (i) high-precision detection, (ii) robustness across LLM backbones, and (iii) computational efficiency.

4 Method

4.1 Overview of MulVul

MulVul operates in two phases: offline preparation and online detection.

During offline preparation, MulVul first constructs a vulnerability knowledge base \mathcal{K} by converting labeled samples into SCALE representations (Wen et al., 2024). MulVul then employs cross-model prompt evolution to optimize prompts for Router and Detector agents. Specifically, we use two separate LLMs with distinct roles: a generator LLM \mathcal{M}_{evo} (e.g., Claude) that proposes and mutates candidate prompts, and an executor LLM $\mathcal{M}_{\text{exec}}$ (e.g., GPT-4o) that runs the Router/Detector agents and returns performance feedback. Through this process, the Router agent obtains a prompt optimized for category-level recall, while each Detector agent receives a prompt tailored for precise fine-grained identification.

During online detection, MulVul adopts a coarse-to-fine Router-Detector architecture, as illustrated

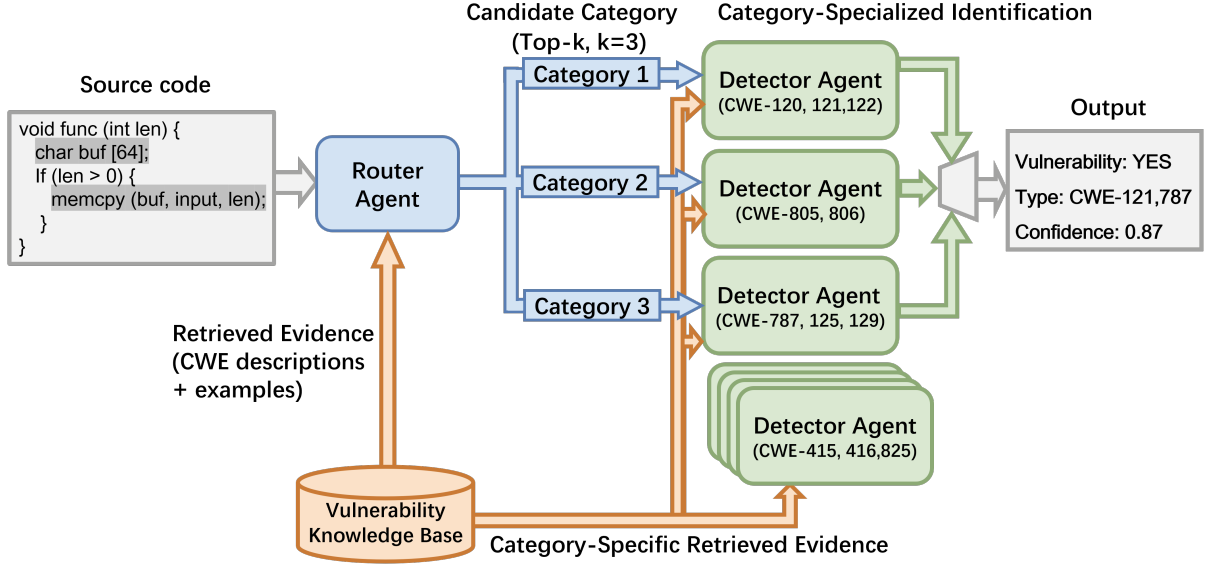


Figure 2: Overview of MulVul for vulnerability detection. The router agent first selects top- k candidate vulnerability categories, and category-specific detector agents then perform fine-grained identification with retrieved CWE-specific evidence.

in Figure 2. Given a code snippet x , a Router agent first actively invokes an analysis tool to retrieve evidence from \mathcal{K} and predicts the top- k categories. Only the corresponding Detector agents are then invoked, each employing specialized contrastive retrieval tools to identify the exact vulnerability. Each Detector operates in isolation without inter-agent communication, avoiding error amplification.

4.2 Offline Preparation

The offline phase 1) constructs the retrieval infrastructure and 2) optimizes prompts for Router and Detector agents.

4.2.1 Knowledge Base Construction

We construct a vulnerability knowledge base \mathcal{K} to provide grounding evidence for both Router and Detector agents. Given the training set $\mathcal{D}_{tr} = \{(x_i, y_i)\}_{i=1}^N$ where x_i is a code snippet and $y_i \in \mathcal{Y}$ is its vulnerability label, we convert each sample into its SCALE representation $T(x_i)$ following (Wen et al., 2024). We index all transformed samples to form the knowledge base:

$$\mathcal{K} = \{(T(x_i), y_i)\}_{i=1}^N \quad (1)$$

For efficient retrieval, we embed each SCALE representation $T(x_i)$ with UniXcoder (Guo et al., 2022) and perform nearest-neighbor search by cosine similarity. We partition the knowledge base into a clean pool \mathcal{K}_0 (entries labeled y_0) and category-specific vulnerability pools $\{\mathcal{K}_m\}_{m=1}^M$

(entries whose CWE category is c_m , i.e., $\mathcal{K}_m = \{(T(x_i), y_i) \in \mathcal{K} \mid y_i \in \mathcal{Y}_m\}$). For Detector m , we denote $\mathcal{K}_{-m} = \bigcup_{j \neq m} \mathcal{K}_j$ as the set of out-of-category vulnerabilities.

During detection, the Router agent invokes the global retrieval tool to access evidence across categories, while each Detector agent employs the contrastive tool to source in-category and hard-negative examples. During the training phases (Stage I and II), when retrieving evidence for a training sample $x_i \in \mathcal{D}_{tr}$, we strictly exclude x_i itself to prevent data leakage.

4.2.2 Cross-Model Prompt Evolution

As illustrated in Figure 3, the key idea is to decouple prompt generation from execution across different LLMs: an evolution model \mathcal{M}_{evo} generates and refines candidate prompts, while an execution model \mathcal{M}_{exec} evaluates them on the detection task. Both \mathcal{M}_{evo} and \mathcal{M}_{exec} remain frozen throughout the optimization process; only the textual prompts are evolved. This separation enhances exploration of the prompt space: since \mathcal{M}_{evo} and \mathcal{M}_{exec} have different internal biases, mutations proposed by \mathcal{M}_{evo} are less likely to exploit superficial patterns, reducing premature convergence to locally optimal prompts.

Algorithm 1 presents the optimization procedure, which proceeds in two stages. Router optimizes Recall@ k for coverage; Detectors optimize F1 for precision-recall balance.

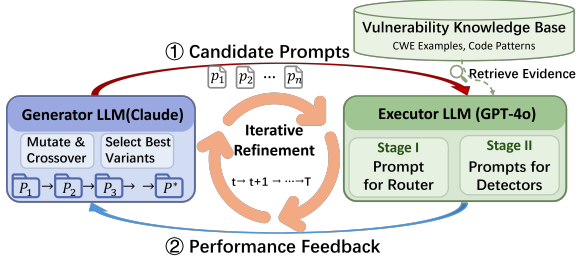


Figure 3: Illustration of the Cross-Model Prompt Evolution Process. The generator LLM \mathcal{M}_{evo} (Claude) proposes and mutates prompts, while the executor LLM $\mathcal{M}_{\text{exec}}$ (GPT-4o) evaluates their fitness.

Stage I: Router Prompt Optimization. We initialize n candidate prompts \mathcal{P}_R using manually designed templates that specify the task format and output structure. In each generation, every prompt $p \in \mathcal{P}_R$ is executed by $\mathcal{M}_{\text{exec}}$ on training samples with retrieved evidence from \mathcal{K} . We use $\text{Recall}@k$ as the fitness function because the Router aims to ensure the correct category is included in top- k predictions, avoiding early filtering of true vulnerabilities. The evolution model \mathcal{M}_{evo} then evolves the prompts through the EVOLVE procedure (Algorithm 2): high-fitness prompts are retained, and new candidates are generated via LLM-driven mutation (e.g., rephrasing instructions, adding constraints, adjusting output format). Throughout evolution, fitness is computed on the training set \mathcal{D}_{tr} . After all iterations are complete, we evaluate each generation’s best prompt (tracked during training) on the held-out validation set \mathcal{D}_{val} , and select the one with the highest $\text{Recall}@k$ as p_R^* .

Stage II: Detector Prompt Optimization. We optimize each Detector prompt independently and in parallel. For category c_m , we construct $\mathcal{D}_{tr}^{(m)}$ and $\mathcal{D}_{val}^{(m)}$ with in-category positives, clean negatives, and out-of-category vulnerabilities (hard negatives). Each Detector is evaluated with F1 score using evidence from \mathcal{K}_m (positives), \mathcal{K}_0 (clean), and \mathcal{K}_{-m} (other categories). The evolution mirrors Stage I, and parallelization across M categories ensures efficiency.

4.3 Online Multi-Agent Detection

Following the two-level CWE hierarchy defined in Section 3.1, MulVul employs a coarse-to-fine detection strategy where autonomous agents are equipped with specialized analysis and retrieval tools to ground their decision-making. Figure 2 illustrates this tool-augmented architecture.

Algorithm 1 Cross-Model Prompt Evolution

Require: \mathcal{M}_{evo} , $\mathcal{M}_{\text{exec}}$, \mathcal{K} , \mathcal{D}_{tr} , \mathcal{D}_{val} , Categories M , Iterations T

Ensure: Optimized prompts p_R^* , $\{p_m^*\}_{m=1}^M$

// Stage I: Router Prompt Optimization

1: Initialize prompts $\mathcal{P}_R \leftarrow \{p_1, \dots, p_n\}$

2: **for** $t = 1$ to T **do**

3: $\mathcal{S} \leftarrow \{\text{Recall}@k(p, \mathcal{M}_{\text{exec}}, \mathcal{D}_{tr}) \mid p \in \mathcal{P}_R\}$

4: $\mathcal{P}_R \leftarrow \text{EVOLVE}(\mathcal{P}_R, \mathcal{S}, \mathcal{M}_{\text{evo}})$

5: Track best prompt $p_{\text{best}}^{(t)}$ based on \mathcal{S}

6: **end for**

7: Let $\mathcal{P}_{\text{best}} = \{p_{\text{best}}^{(1)}, \dots, p_{\text{best}}^{(T)}\}$

8: $p_R^* \leftarrow \arg \max_{p \in \mathcal{P}_{\text{best}}} \text{Recall}@k(p, \mathcal{M}_{\text{exec}}, \mathcal{D}_{val})$

▷ Final Selection on Val

// Stage II: Detector Prompt Optimization

9: **for** $m = 1$ to M **in parallel do**

10: Initialize \mathcal{P}_m ; Construct $\mathcal{D}_{tr}^{(m)}$, $\mathcal{D}_{val}^{(m)}$

11: **for** $t = 1$ to T **do**

12: $\mathcal{S} \leftarrow \{\text{F1}(p, m, \mathcal{M}_{\text{exec}}, \mathcal{D}_{tr}^{(m)}) \mid p \in \mathcal{P}_m\}$

13: $\mathcal{P}_m \leftarrow \text{EVOLVE}(\mathcal{P}_m, \mathcal{S}, \mathcal{M}_{\text{evo}})$

14: **end for**

15: Select p_m^* using $\mathcal{D}_{val}^{(m)}$ from evolved candidates

16: **end for**

17: **return** p_R^* , $\{p_m^*\}_{m=1}^M$

Given the optimized prompts p_R^* and $\{p_m^*\}_{m=1}^M$ from offline preparation, MulVul performs retrieval-augmented multi-agent detection at inference time. Algorithm 3 summarizes the procedure.

4.3.1 Router agent: Global Planning

Given an input code snippet x , the Router agent acts as a dispatcher to predict coarse-grained categories. To overcome the limitations of raw text processing, the agent first employs a Structure Analysis Tool (SCALE) to extract semantic features:

$$T(x) = \text{TOOL}_{\text{SCALE}}(x) \quad (2)$$

With this structured representation, the agent actively invokes a Global Retrieval Tool to query the knowledge base \mathcal{K} for r cross-category examples:

$$E_R = \text{TOOL}_{\text{Global}}(T(x), \mathcal{K}, r). \quad (3)$$

The Router agent utilizes these top- r retrieved examples to understand the broad semantic context. The Router agent then takes the optimized prompt p_R^* , the original code x , and evidence E_R as input,

Algorithm 2 EVOLVE: LLM-Driven Prompt Evolution

Require: Population \mathcal{P} , Fitness scores $\{\mathcal{F}(p)\}_{p \in \mathcal{P}}$, Evolution model \mathcal{M}_{evo} , Elite ratio α

Ensure: Updated prompts \mathcal{P}'

- 1: $\mathcal{P}' \leftarrow \text{top-}[\alpha|\mathcal{P}|]$ prompts ranked by \mathcal{F}
 - 2: **while** $|\mathcal{P}'| < |\mathcal{P}|$ **do**
 - 3: Sample p via rank-based selection to maintain diversity
 - 4: $p' \leftarrow \mathcal{M}_{\text{evo}}(\text{mutate}, p, \mathcal{F}(p))$
 - 5: $\mathcal{P}' \leftarrow \mathcal{P}' \cup \{p'\}$
 - 6: **end while**
 - 7: **return** \mathcal{P}'
-

379 and outputs a ranked list of top- k category predic-
380 tions:

$$381 \quad \mathcal{C}_{\text{top-}k} = \text{ROUTER}(p_R^*, x, E_R) \quad (4)$$

382 4.3.2 Detector agents: Fine-grained 383 Identification

384 For each predicted category $c_m \in \mathcal{C}_{\text{top-}k}$, the cor-
385 responding Detector agent performs fine-grained
386 vulnerability type identification. To prevent confir-
387 mation bias, the Detector agent is equipped with
388 a Contrastive Retrieval Tool. This tool dynam-
389 ically sources evidence from three distinct pools:
390 in-category positives \mathcal{K}_m , clean examples \mathcal{K}_0 , and
391 out-of-category hard negatives \mathcal{K}_{-m} . The agent al-
392 locates its retrieval budget as $r_{\text{pos}} = r_{\text{neg}} = \lfloor r/3 \rfloor$
393 and $r_{\text{hard}} = r - r_{\text{pos}} - r_{\text{neg}}$.

394 Based on this allocation, the agent invokes the
395 tool to construct the context:

$$396 \quad E_m = \text{TOOL}_{\text{Contrast}}(T(x), c_m, \mathcal{K}, r) \quad (5)$$

397 Each Detector agent then analyzes this contrastive
398 context to produce a prediction:

$$399 \quad (\hat{\mathcal{Y}}_m, \hat{\mathcal{E}}_m) = \text{DETECTOR}_m(p_m^*, x, E_m) \quad (6)$$

400 where $\hat{\mathcal{Y}}_m$ represents the identified vulnerability
401 types and $\hat{\mathcal{E}}_m$ contains the explanations. By op-
402 erating with isolated tools, the agents avoid error
403 cascading. After all invoked Detector agents re-
404 turn their predictions, MulVul aggregates them to
405 produce the final output.

406 5 Evaluation

407 We evaluate MulVul through comprehensive exper-
408 iments designed to answer the following questions:

Algorithm 3 MulVul Online Detection

Require: Code snippet x , Knowledge base \mathcal{K} , Cat-
egory subsets $\{\mathcal{K}_m\}_{m=1}^M$, Router prompt p_R^* ,
Detector prompts $\{p_m^*\}_{m=1}^M$

Ensure: Prediction $\hat{\mathcal{Y}}$, Evidence $\hat{\mathcal{E}}$

// Phase I: Coarse-grained Routing

- 1: $T(x) \leftarrow \text{TOOL}_{\text{SCALE}}(x) \triangleright$ Structure Analysis
- 2: $E_R \leftarrow \text{TOOL}_{\text{Global}}(T(x), \mathcal{K}, r)$
- 3: $\mathcal{C}_{\text{top-}k} \leftarrow \text{ROUTER}(p_R^*, x, E_R)$

// Phase II: Fine-grained Detection

- 4: $\hat{\mathcal{Y}} \leftarrow \emptyset; \hat{\mathcal{E}} \leftarrow \emptyset$
 - 5: **for** $c_m \in \mathcal{C}_{\text{top-}k}$ **in parallel do**
 - 6: **// Detector invokes contrastive tool**
 - 7: $E_m \leftarrow \text{TOOL}_{\text{Contrast}}(T(x), m, \mathcal{K}, r)$
 - 8: $(\hat{\mathcal{Y}}_m, \hat{\mathcal{E}}_m) \leftarrow \text{DETECTOR}_m(p_m^*, x, E_m)$
 - 9: $\hat{\mathcal{Y}} \leftarrow \hat{\mathcal{Y}} \cup \hat{\mathcal{Y}}_m$
 - 10: $\hat{\mathcal{E}} \leftarrow \hat{\mathcal{E}} \cup \hat{\mathcal{E}}_m$
 - 11: **end for**
 - // Phase III: Aggregation**
 - 12: **if** $\hat{\mathcal{Y}} = \emptyset$ **then**
 - 13: $\hat{\mathcal{Y}} \leftarrow \{y_0\}$
 - 14: **end if**
 - 15: **return** $\hat{\mathcal{Y}}, \hat{\mathcal{E}}$
-

- **Q1:** How does MulVul compare with existing 409
LLM-based vulnerability detection methods? 410
- **Q2:** How does the routing parameter k affect 411
the precision-recall trade-off? 412
- **Q3:** How do different components contribute 413
to MulVul’s performance? 414
- **Q4:** How does MulVul perform on few-shot 415
CWE types? 416

5.1 Experimental Setup 417

Dataset. We evaluate on PrimeVul (Ding et al., 418
2024), containing 6,968 vulnerable and 229,764 419
benign C/C++ functions across 10 categories and 420
130 CWE types. 421

Implementation. We use GPT-4o as the execu- 422
tion model $\mathcal{M}_{\text{exec}}$ for both Router and Detector 423
agents, and Claude Opus 4.5 as the evolution model 424
 \mathcal{M}_{evo} . We use UniXcoder (Guo et al., 2022) for 425
embedding and FAISS for retrieval. 426

Metrics. Following Ding et al. (2024), we re- 427
port Macro-Precision, Macro-Recall, and Macro- 428
F1. Macro-averaging computes metrics indepen- 429
dently for each CWE type and then averages them, 430

ensuring equal weight for all types and avoiding dominance by high-frequency vulnerabilities under severe class imbalance.

Baselines. We compare our approach with four state-of-the-art methods that span prompting, fine-tuning, and GNN paradigms. 1) GPT-4o: Prompting-based detection without demonstration examples or fine-tuning. 2) LLM×CPG (Lekssays et al., 2025): LoRA fine-tuned Qwen2.5-32B with CPG-guided context. 3) LLMVulExp (Mao et al., 2025): LoRA fine-tuned CodeLlama-7B with chain-of-thought explanations. 4) VISION (Egea et al., 2025): Devign GNN with counterfactual augmentation. LLM×CPG and VISION are extended from binary to multi-class classification for fair comparison.

5.2 Comparison of Vulnerability Detection Effectiveness (Q1)

We compare the vulnerability detection effectiveness of MulVul with existing methods at the coarse-grained category level and fine-grained type level.

Category-Level Detection. Table 1 reports category-level results. MulVul achieves the best overall performance with 50.41% Macro-F1, outperforming the strongest baseline LLMVulExp by 8.91 points. MulVul also achieves the highest Macro-Precision (44.31%) while maintaining strong Macro-Recall (58.45%), indicating accurate category identification with fewer false positives. By contrast, LLM×CPG yields the highest recall (62.81%) but substantially lower precision (27.44%), suggesting that expanding candidates improves coverage but induces over-prediction.

Method	Macro-Precision	Macro-Recall	Macro-F1
GPT-4o	22.20	13.13	16.50
LLM×CPG	27.44	62.81	38.20
LLMVulExp	37.88	45.88	41.50
VISION	22.23	33.72	26.80
MulVul (Ours)	44.31	58.45	50.41

Table 1: Category-level vulnerability detection effectiveness (%) on PrimeVul.

Type-Level Detection. Table 2 presents type-level results. The task is markedly harder: all baselines exhibit a sharp precision drop, reflecting that fine-grained types require discriminative evidence beyond generic vulnerability semantics. MulVul achieves 34.79% Macro-F1, surpassing LLM×CPG by 10.21 points. Importantly, MulVul

improves Macro-Precision to 27.90% while keeping competitive Macro-Recall, yielding a stronger precision–recall trade-off that is critical for practical deployment.

Method	Macro-Precision	Macro-Recall	Macro-F1
GPT-4o	4.76	3.28	3.86
LLM×CPG	16.80	45.80	24.58
LLMVulExp	19.31	27.60	22.72
VISION	14.91	23.12	18.12
MulVul (Ours)	27.90	46.19	34.79

Table 2: Type-level vulnerability detection effectiveness (%) on PrimeVul.

5.3 Impact of Routing Parameter k (Q2)

The routing parameter k controls the number of candidate categories the Router passes to downstream Detectors, directly affecting the precision-recall trade-off.

Top- k	Macro-Precision	Macro-Recall	Macro-F1
1	39.58	29.10	33.51
2	28.80	43.20	34.56
3	27.90	46.19	34.79
4	26.79	47.83	34.34
5	26.54	48.37	34.27

Table 3: Effect of routing parameter k on PrimeVul (Type-level, %).

Analysis. We observe three key patterns. First, Macro-Recall consistently increases as k grows. This indicates that allowing the Router to activate multiple candidate categories substantially reduces missed detections, as the true class is more likely to be covered by the expanded Top- k set. Second, Macro-Precision shows a clear downward trend with larger k . As more detectors are triggered, incorrect categories are increasingly introduced, leading to more false positives and thus lower precision. This behavior reflects the inherent trade-off between coverage and noise when expanding the routing space. Third, Macro-F1 reaches its peak at $k=3$ and remains relatively stable beyond this range. Although recall continues to improve for larger k , the corresponding degradation in precision offsets these gains, resulting in diminishing overall benefits.

5.4 Ablation Study (Q3)

To understand the contribution of each component in MulVul, we conduct ablation studies by removing key modules. Table 4 presents the results.

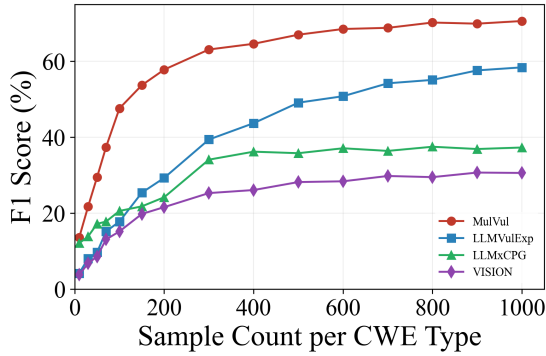


Figure 4: F1 score vs. CWE sample count. MulVul outperforms baselines across all data regimes, with the largest gains on few-shot CWEs.

Variant	RAG	Agents	Evolution	Macro-F1	Δ
GPT-4o	✗	✗	✗	3.86	-30.70
w/o Retrieval	✗	✓	✓	21.80	-12.76
w/o Agents	✓	✗	✓	28.61	-5.95
w/o Evolution	✓	✓	✗	22.80	-11.76
MulVul (Full)	✓	✓	✓	34.56	-

Table 4: Ablation study on PrimeVul (Type-level). Δ denotes the Macro-F1 difference from the full model.

Analysis. Retrieval augmentation is the most critical component. Removing evidence retrieval causes the largest performance drop, reducing Macro-F1 from 34.56% to 21.80%. This confirms that grounding LLM reasoning with retrieved vulnerability examples from the knowledge base \mathcal{K} is essential for distinguishing semantically similar CWE types. Without concrete code evidence, even well-structured prompts and specialized agents struggle to make accurate fine-grained predictions. Moreover, cross-model prompt evolution provides substantial gains. Replacing evolved prompts with manual templates leads to an 11.76% F1 drop, demonstrating that our cross-model evolution strategy (Section 4.2) effectively optimizes task-specific instructions.

5.5 Performance on Few-Shot CWE Types (Q4)

Real-world vulnerability datasets exhibit severe class imbalance, with many CWE types having only a small number of samples (i.e., few-shot settings). We analyze how methods perform across CWEs grouped by sample count. Figure 4 visualizes the relationship between CWE sample size and detection performance.

Analysis. First, MulVul has a strong few-shot performance. For CWEs with fewer than 100 samples, MulVul achieves approximately 48% F1, nearly doubling the performance of the best baseline LLMVulExp (25%). This demonstrates that retrieval augmentation enables effective cross-CWE knowledge transfer. Similar vulnerability patterns from related types provide useful detection signals even when target-type samples are scarce.

Second, MulVul’s performance curve rises steeply and plateaus around 300 samples at approximately 63% F1, while fine-tuning methods (LLM \times CPG, VISION) plateau much earlier at lower performance levels (35-38%). This indicates that MulVul extracts more discriminative information from limited samples, a crucial advantage for practical deployment where many vulnerability types are inherently rare.

Third, the advantage persists in data-rich regimes. Even for CWE types with over 500 samples, MulVul maintains a 12+ point F1 lead over baselines. This demonstrates that MulVul’s coarse-to-fine strategy and architecture are all more beneficial than existing schemes.

See Appendix A for per-CWE analysis and quantitative few-shot metrics.

6 Conclusion

We propose MulVul, a retrieval-augmented multi-agent framework for vulnerability detection. The coarse-to-fine Router-Detector architecture addresses the heterogeneity and scalability challenges in analyzing massive weakness categories. Additionally, cross-model prompt evolution automates the discovery of specialized instructions while mitigating self-correction bias, and SCALE-based contrastive retrieval grounds LLM reasoning. Experiments on PrimeVul demonstrate that MulVul achieves a state-of-the-art 34.79% Macro-F1 (41.5% relative improvement), and our evolutionary mechanism yields a 51.6% performance boost over manual prompt engineering.

568 Limitations

569 We acknowledge several limitations of our work:

- 570 • MulVul is evaluated exclusively on Prime-
571 Vul containing C/C++ code. Effectiveness
572 on other programming languages (e.g., Java,
573 Python) with different vulnerability patterns
574 and on other benchmarks remains unexplored.
- 575 • MulVul requires multiple LLM API calls: iter-
576 ative optimization during offline prompt evolu-
577 tion and $1 + k$ calls per sample during on-
578 line detection. This may limit applicability
579 in resource-constrained or large-scale batch
580 processing scenarios.
- 581 • Although we claim that cross-model evolu-
582 tion improves generalization, our experiments
583 primarily use GPT-4o as the execution model.
584 The transferability of evolved prompts to other
585 LLMs was not thoroughly evaluated due to
586 scope constraints.
- 587 • We recognize the potential for misuse associ-
588 ated with automated vulnerability detection
589 tools. While MulVul is designed to aid devel-
590 opers in securing code, malicious actors could
591 theoretically utilize the framework to discover
592 zero-day vulnerabilities in software systems
593 for exploitation. Furthermore, there is a risk
594 of automation bias; developers might develop
595 a false sense of security and reduce manual
596 scrutiny, which is dangerous given that our
597 model inevitably produces false negatives.

598 References

599 Saikat Chakraborty, Rahul Krishna, Yangruibo Ding,
600 and Baishakhi Ray. 2021. Deep learning based vul-
601 nerability detection: Are we there yet? *IEEE Trans-*
602 *actions on Software Engineering*, 48(9):3280–3296.

603 Yangruibo Ding, Yanjun Fu, Omniyyah Ibrahim,
604 Chawin Sitawarin, Xinyun Chen, Basel Alomair,
605 David Wagner, Baishakhi Ray, and Yizheng Chen.
606 2024. Vulnerability detection with code language
607 models: How far are we? In *2025 IEEE/ACM 47th*
608 *International Conference on Software Engineering*
609 *(ICSE)*, pages 469–481. IEEE Computer Society.

610 David Egea, Barproda Halder, and Sanghamitra Dutta.
611 2025. Vision: Robust and interpretable code vulner-
612 ability detection leveraging counterfactual augmen-
613 tation. In *Proceedings of the AAAI/ACM Conference*
614 *on AI, Ethics, and Society*, volume 8, pages 812–
615 823.

Jun Gao, Yun Peng, and Xiaoxue Ren. 2025. \texttt
{ReMind}: Understanding deductive code reason-
ing in llms. *arXiv preprint arXiv:2511.00488*. 616
617
618

Seyed Mohammad Ghaffarian and Hamid Reza Shahri-
ari. 2017. Software vulnerability analysis and
discovery using machine-learning and data-mining
techniques: A survey. *ACM computing surveys*
(*CSUR*), 50(4):1–36. 619
620
621
622
623

Daya Guo, Shuai Lu, Nan Duan, Yanlin Wang, Ming
Zhou, and Jian Yin. 2022. Unixcoder: Unified cross-
modal pre-training for code representation. In *Pro-*
ceedings of the 60th Annual Meeting of the Associa-
tion for Computational Linguistics (Volume 1: Long
Papers), pages 7212–7225. 624
625
626
627
628
629

Daya Guo, Shuo Ren, Shuai Lu, Zhangyin Feng,
Duyu Tang, Shujie LIU, Long Zhou, Nan Duan,
Alexey Svyatkovskiy, Shengyu Fu, and 1 others.
2021. Graphcodebert: Pre-training code represen-
tations with data flow. In *International Conference*
on Learning Representations. 630
631
632
633
634
635

Qingyan Guo, Rui Wang, Junliang Guo, Bei Li, Kaitao
Song, Xu Tan, Guoqing Liu, Jiang Bian, and Yujiu
Yang. 2024. Connecting large language models with
evolutionary algorithms yields powerful prompt op-
timizers. In *The Twelfth International Conference*
on Learning Representations. 636
637
638
639
640
641

Sirui Hong, Mingchen Zhuge, Jonathan Chen, Xiawu
Zheng, Yuheng Cheng, Jinlin Wang, Ceyao Zhang,
Zili Wang, Steven Ka Shing Yau, Zijuan Lin, and
1 others. 2023. Metagpt: Meta programming for a
multi-agent collaborative framework. In *The Twelfth*
International Conference on Learning Representa-
tions. 642
643
644
645
646
647
648

Ahmed Lekssays, Hamza Mouhcine, Khang Tran, Ting
Yu, and Issa Khalil. 2025. {LLMxCPG}:{Context-
Aware} vulnerability detection through code prop-
erty {Graph-Guided} large language models. In
34th USENIX Security Symposium (USENIX Secu-
rity 25), pages 489–507. 649
650
651
652
653
654

Patrick Lewis, Ethan Perez, Aleksandra Piktus, Fabio
Petroni, Vladimir Karpukhin, Naman Goyal, Hein-
rich Küttler, Mike Lewis, Wen-tau Yih, Tim Rock-
täschel, and 1 others. 2020. Retrieval-augmented
generation for knowledge-intensive nlp tasks. *Ad-*
vances in neural information processing systems,
33:9459–9474. 655
656
657
658
659
660
661

Zhen Li, Deqing Zou, Shouhuai Xu, Hai Jin, Yawei
Zhu, and Zhaoxuan Chen. 2021. Sysevr: A frame-
work for using deep learning to detect software vul-
nerabilities. *IEEE Transactions on Dependable and*
Secure Computing, 19(4):2244–2258. 662
663
664
665
666

Zhen Li, Deqing Zou, Shouhuai Xu, Xinyu Ou, Hai
Jin, Sujuan Wang, Zhijun Deng, and Yuyi Zhong.
2018. Vuldeepecker: A deep learning-based system
for vulnerability detection. In *25th Annual Network*
and Distributed System Security Symposium, NDSS
2018, San Diego, California, USA, February 18-21,
2018. The Internet Society. 667
668
669
670
671
672
673

674	Jie Lin and David Mohaisen. 2025. From large to mammoth: A comparative evaluation of large language models in vulnerability detection. In <i>Proceedings of the 2025 Network and Distributed System Security Symposium (NDSS)</i> .	Xin Zhou, Sicong Cao, Xiaobing Sun, and David Lo. 2025. Large language model for vulnerability detection and repair: Literature review and the road ahead. <i>ACM Transactions on Software Engineering and Methodology</i> , 34(5):1–31.	731
675			732
676			733
677			734
678			735
679	Shuai Lu, Nan Duan, Hojae Han, Daya Guo, Seungwon Hwang, and Alexey Svyatkovskiy. 2022. Reacc: A retrieval-augmented code completion framework. In <i>Proceedings of the 60th Annual Meeting of the Association for Computational Linguistics (Volume 1: Long Papers)</i> , pages 6227–6240.	Yaqin Zhou, Shangqing Liu, Jingkai Siow, Xiaoning Du, and Yang Liu. 2019. Devign: Effective vulnerability identification by learning comprehensive program semantics via graph neural networks. <i>Advances in neural information processing systems</i> , 32.	736
680			737
681			738
682			739
683			740
684			
685	Qiheng Mao, Zhenhao Li, Xing Hu, Kui Liu, Xin Xia, and Jianling Sun. 2025. Towards explainable vulnerability detection with large language models. <i>IEEE Transactions on Software Engineering</i> .	Yongchao Zhou, Andrei Ioan Muresanu, Ziwen Han, Keiran Paster, Silviu Pitis, Harris Chan, and Jimmy Ba. 2022. Large language models are human-level prompt engineers. In <i>The eleventh international conference on learning representations</i> .	741
686			742
687			743
688			744
689	MITRE. 2024. CWE List Version 4.19. https://cwe.mitre.org/data/index.html . Page last updated: November 19, 2024. Accessed: 2026-01-01.		745
690			
691			
692	Yun Peng, Shuzheng Gao, Cuiyun Gao, Yintong Huo, and Michael Lyu. 2024. Domain knowledge matters: Improving prompts with fix templates for repairing python type errors. In <i>Proceedings of the 46th IEEE/ACM international conference on software engineering</i> , pages 1–13.		
693			
694			
695			
696			
697			
698	Yun Peng, Kisub Kim, Linghan Meng, and Kui Liu. 2025. icodereviewer: Improving secure code review with mixture of prompts. In <i>Proceedings of the 40th IEEE/ACM International Conference on Automated Software Engineering</i> .		
699			
700			
701			
702			
703	Ze Sheng, Zhicheng Chen, Shuning Gu, Heqing Huang, Guofei Gu, and Jeff Huang. 2025. LLMs in Software Security: A Survey of Vulnerability Detection Techniques and Insights. <i>ACM Computing Surveys</i> , 58(5):1–35.		
704			
705			
706			
707			
708	Jason Wei, Xuezhi Wang, Dale Schuurmans, Maarten Bosma, Fei Xia, Ed Chi, Quoc V Le, Denny Zhou, and 1 others. 2022. Chain-of-thought prompting elicits reasoning in large language models. <i>Advances in neural information processing systems</i> , 35:24824–24837.		
709			
710			
711			
712			
713			
714	Xin-Cheng Wen, Cuiyun Gao, Shuzheng Gao, Yang Xiao, and Michael R Lyu. 2024. Scale: Constructing structured natural language comment trees for software vulnerability detection. In <i>Proceedings of the 33rd ACM SIGSOFT International Symposium on Software Testing and Analysis</i> , pages 235–247.		
715			
716			
717			
718			
719			
720	Qingyun Wu, Gagan Bansal, Jieyu Zhang, Yiran Wu, Beibin Li, Erkang Zhu, Li Jiang, Xiaoyun Zhang, Shaokun Zhang, Jiale Liu, and 1 others. 2024. Auto-gen: Enabling next-gen llm applications via multi-agent conversations. In <i>First Conference on Language Modeling</i> .		
721			
722			
723			
724			
725			
726	Chengrun Yang, Xuezhi Wang, Yifeng Lu, Hanxiao Liu, Quoc V Le, Denny Zhou, and Xinyun Chen. 2023. Large language models as optimizers. In <i>The Twelfth International Conference on Learning Representations</i> .		
727			
728			
729			
730			

A Few-Shot CWE Performance Analysis

This appendix provides a detailed analysis of detection performance on individual CWE types, complementing the aggregated results in Section 5.5. We examine how class imbalance affects each method and quantify MulVul’s advantages on few-shot CWE types, i.e., those with limited training samples.

A.1 Class Imbalance in PrimeVul

Table 5 characterizes the dataset’s long-tail distribution: 69.6% of samples concentrate in only 12 CWE types, while 48 types (37% of all CWEs) collectively contain less than 1% of samples. This severe imbalance creates few-shot scenarios for many CWE types, where models must generalize from extremely limited examples.

Tier	#CWEs	Samples	Share
Head ($\geq 5k$)	12	140,080	69.6%
Medium (1k–5k)	16	42,554	21.2%
Low (100–1k)	54	16,735	8.3%
Rare (50–100)	16	1,109	0.6%
Very Rare (10–50)	25	656	0.3%
Ext. Rare (< 10)	7	32	$< 0.1\%$
Total	130	201,166	100%

Table 5: CWE distribution in PrimeVul. The bottom four tiers (48 CWE types) represent few-shot scenarios with < 100 samples each.

A.2 Per-CWE Performance Visualization

Figure 5 plots each method’s F1 on every CWE type against its sample count. This visualization reveals how performance scales with data availability and identifies which methods handle few-shot CWEs effectively.

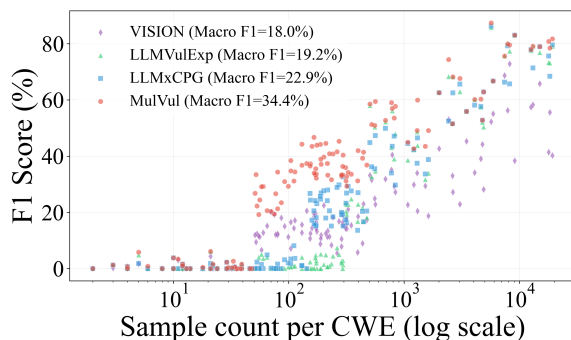


Figure 5: Per-CWE F1 vs. sample count (log scale). MulVul (red) consistently outperforms baselines, especially in the few-shot region (left).

A.3 Few-Shot Performance Metrics

To quantify the few-shot detection capability, we define four metrics focusing on CWE types with < 500 samples. Table 6 presents the results.

Metric	MulVul	LLM×CPG	VulExp	VISION
Tail F1 \uparrow	0.228	0.095	0.036	0.094
Fail Thresh. \downarrow	51	153	311	51
Tail Cov. \uparrow	65.6%	40.9%	11.8%	55.9%
Gini Coef. \downarrow	0.396	0.580	0.695	0.495

Table 6: Few-shot performance metrics (\uparrow : higher is better; \downarrow : lower is better). VulExp = LLMVulExp.

Metric Definitions:

- *Few-Shot F1*: Average F1 on CWEs with < 500 samples.
- *Min. Samples*: Minimum samples needed for F1 > 0 (data efficiency).
- *Coverage*: Fraction of few-shot CWEs achieving F1 > 0.1 (detection breadth).
- *Gini Coefficient*: F1 distribution inequality across CWEs (0 = uniform, 1 = skewed).

Analysis First, MulVul achieves the highest few-shot F1. MulVul achieves 0.228 F1 on few-shot CWEs, which is $2.4\times$ higher than LLM×CPG (0.095) and $6.3\times$ higher than LLMVulExp (0.036). This confirms that retrieval augmentation enables cross-CWE knowledge transfer: when a CWE type has few samples, MulVul leverages similar patterns from the knowledge base. In contrast, fine-tuning methods need substantial data to learn discriminative features, while retrieval-based methods generalize from analogous examples.

Moreover, MulVul shows the most balanced performance. The Gini coefficient measures how uniformly F1 scores are distributed across CWE types. MulVul’s lowest Gini (0.396) indicates consistent performance regardless of class frequency, while LLMVulExp’s high Gini (0.695) reveals heavy bias toward frequent classes. This balance is essential for Macro-F1 optimization under class imbalance.

B Case Study: Impact of Prompt Evolution

To analyze how MulVul improves prompt robustness, Figure 6 visually contrasts the manually designed prompt (Stage 0) with the final evolved prompt (Stage T).

First, MulVul enables a shift from implicit to explicit definitions. As shown in Figure 6(a), the

Initial Prompt (Manual Design)

Role: You are a security expert specializing in detecting coding vulnerabilities.

Instructions:

1. Identify which patterns from the evidence examples appear in the target code.
2. If the code shares vulnerable patterns with the examples, classify accordingly.
3. Only mark as Benign if NO similar patterns exist.

Categories: Memory, Injection, Logic, Input, Crypto, Benign

Target Code: {code}
Evidence: {evidence}

Output (JSON): { "predictions": [{ "category": "...", "confidence": 0.85, "reason": "..." }] }

(a) Baseline prompt lacks definitions and explicit constraints.

Evolved Prompt (Optimized by MulVul)

Role: You are a **senior security analyst**. Determine vulnerability by **explicitly comparing against confirmed patterns**.

Constraints: - **Do NOT infer vulnerabilities beyond these patterns.**
- **Do NOT speculate about hypothetical vulnerabilities.**

Category Definitions (Key Signals): - *Memory:* Direct memory manipulation **without bounds**.
- *Injection:* User data reaches execution context.
- *Input:* **Distinction: Affects data integrity but does NOT execute code.**
- *Logic:* Code "works as written" but violates security assumptions.

Error Prevention Hints: - **Injection vs Input:** Injection executes instructions; Input flaws only mishandle data.
- **Benign vs Vulnerable:** If no strong pattern match, default to Benign.

Output Format (STRICT JSON): ...

(b) Evolved prompt incorporates negative constraints, disambiguation rules, and specific signals.

Figure 6: Comparison of the Router agent’s prompt before and after Cross-Model Evolution. The **Initial Prompt** (a) relies on generic instructions, while the **Evolved Prompt** (b) introduces semantic disambiguation (e.g., Injection vs. Input) and negative constraints (e.g., “Do NOT speculate”) to mitigate hallucinations. High-impact additions are highlighted in **bold blue**.

initial prompt lists categories without definitions, relying entirely on the LLM’s parametric knowledge. This often leads to confusion between conceptually similar types, such as *Injection* (CWE-74) and *Input Validation* (CWE-20). In contrast, the evolved prompt in Figure 6(b) explicitly injects discriminative boundaries (e.g., “*Input flaws affect data integrity but do NOT execute code*”). This change, driven by the error feedback loop during evolution, significantly improves the Router’s classification precision.

Second, MulVul mitigates false positives through negative constraints. A major challenge in vulnerability detection is the high false positive rate caused by LLMs’ “hallucinating” flaws in benign code. The evolutionary process introduced negative constraints, highlighted in bold blue in Figure 6(b) (e.g., “*Do NOT infer vulnerabilities beyond these patterns*”). These “stop words” act as guardrails, forcing the agent to output *Benign* when evidence is insufficient, thereby reducing the False Positive Rate.

Third, MulVul adds an error prevention mechanism. The evolved prompt includes a novel “*Error*

Prevention Hints” section. This suggests that the Executor LLM (GPT-4o) successfully identified recurring confusion patterns in early iterations and the Generator LLM (Claude) synthesized these observations into explicit “Chain-of-Thought” rules (e.g., *Memory vs. Logic*) to guide future reasoning.

Acknowledgments

We used large language models (Gemini, Claude, and GPT-5.2) to assist with grammar checking, polishing, and improving the clarity of the writing. All technical contributions, experimental design, implementation, and analysis were conducted entirely by the authors. The authors take full responsibility for the content of this paper.